Article No. jmbi.1999.2924 available online at http://www.idealibrary.com on IDEAL® J. Mol. Biol. (1999) 290, 811–822

JMB

Experimental Study of the Protein Folding Landscape: Unfolding Reactions in Cytochrome *c*

John S. Milne, Yujia Xu, Leland C. Mayne and S. Walter Englander*

The Johnson Research Foundation Department of Biochemistry and Biophysics University of Pennsylvania Philadelphia, PA 19104-6059, USA

**Corresponding author*

Hydrogen exchange results for cytochrome *c* have been interpreted in terms of transient hydrogen bond-breaking reactions that include large unfolding reactions and small fluctuational distortions. The differential sensitivity of these opening reactions to denaturant, temperature, and protein stability makes it possible to distinguish the different opening reactions and to characterize their structural and thermodynamic parameters. The partially unfolded forms (PUFs) observed are few and discrete, evidently because they are produced by the reversible unfolding of the protein's several intrinsically cooperative secondary structural elements. The PUFs are robust, evidently because the structural elements do not change over a wide range of conditions. The discrete nature of the PUFs and their small number is as expected for classical folding intermediates but not for theoretically derived folding models apparently because the simplified non-protein models usually analyzed in theoretical studies encompass only a single cooperative unit rather than multiple separable units.

Keywords: cytochrome *c*; protein folding; folding landscape; hydrogen exchange; protein dynamics

Introduction

A great deal of experimental work is consistent with the view that protein folding proceeds through classical pathways defined by relatively discrete intermediates (Kim & Baldwin, 1982, 1990; Creighton, 1990; Ptitsyn, 1995). Alternatively, theoretical analyses of non-protein models picture an unlimited number of continuously distributed intermediates and pathways (Bryngelson *et al.*, 1995; Dill & Chan, 1997; Mirny *et al.*, 1996; Veitshans *et al.*, 1997; Wolynes *et al.*, 1995). Here, we describe an experimental study of the partially folded intermediates that exist in the folding landscape of a real protein. The results suggest an explanation for the divergent descriptions of the landscape based on the different kinds of models studied.

Thermodynamic principles require that protein molecules must continually cycle through all possible states and populate them in a Boltzmann manner. Thus proteins unfold and refold all the time, even under fully native conditions, producing an equilibrium population of intermediates that maps the free energy landscape between the unfolded (U) and native (N) states. The landscape and the folding pathway that it produces might be studied experimentally by characterizing these forms. The problem is that under most conditions the intermediates are only infinitesimally populated, invisible to experimental measurement.

It is possible to study the high-energy protein forms at equilibrium under native conditions by a hydrogen exchange (HX) method. The method works in principle because, unlike other methods, the overwhelmingly populated native state makes no contribution to the HX signals that one measures. Measurable HX is wholly determined by the thermodynamic cycling of protein molecules through higher energy intermediate forms in which protecting H-bonds present in the native state are transiently broken, allowing attack by HX catalysts (OH^- and H^+ plus associated water molecules).

A practical problem arises. In stable proteins the exchange of many protected hydrogen atoms is often dominated by small fluctuations that break only one hydrogen bond at a time (Milne *et al.*,

Abbreviations used: cyt *c*, cytochrome *c* (equine); HX, hydrogen exchange; N, native state; U, globally unfolded state; PUF, partially unfolded form; T_m, melting temperature; GmCl, guanidinium chloride; GmSCN, guanidinium thiocyanate.

E-mail address of the corresponding author: walter@HX2.Med.UPenn.Edu

0022-2836/99/280811–12 $30.00/0

1998) rather than by the partially unfolded forms (PUFs) that must define the protein folding process. The native state HX method exploits the fact that destabilizing influences selectively promote large unfoldings: not only the global unfolding but also partial unfoldings. The unfolding reactions can then come to dominate the exchange of the many hydrogen atoms that they expose. In favorable cases HX data can then distinguish and identify the PUFs and evaluate their structural and thermodynamic parameters.

Native state HX results for oxidized equine cytochrome *c* (cyt *c*) have been interpreted in terms of the cooperative unfolding units shown in Figure 1 (Bai *et al.*, 1995b). The color-coding represents the increasing free energy level of the unfolded intermediate forms, from red to blue. The present work further explores the equilibrium population of PUFs in the high-energy reaction landscape using denaturant and temperature which affect protein stability in a general way, and the redox state of the heme iron which affects cyt *c* stability in a structurally defined way.

Results

A structurally protected amide hydrogen may exchange with solvent through a variety of protein distortions, ranging from small fluctuational motions that separate a single protecting H-bond through larger unfolding reactions that reach up to the global unfolding. The fastest pathway for any given hydrogen atom will dominate its exchange. We are interested in the ability of various conditions to selectively unmask or suppress the competing HX pathways. The results shown below probe the HX sensitivities of over 40 hydrogen atoms distributed throughout cyt *c*.

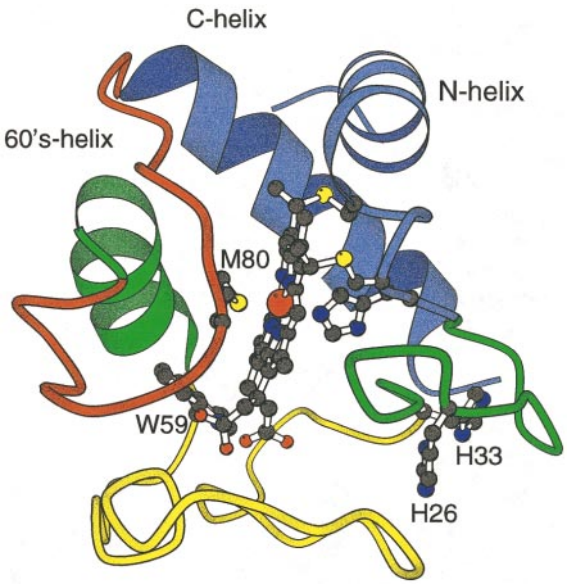

Figure 1. Cytochrome *c*. Equine cyt *c* is a small molecule of 104 residues folded into three major helices and three major omega loops, with a covalently bound heme group. The cooperative unfolding units discussed here are shown in color, with unfolding free energy increasing in the order red to yellow to green to blue.

Dependence of HX rates on denaturant

Figures 2 and 3 show HX results for oxidized cyt *c* (left) as a function of guanidinium chloride (GmCl) concentration and for the more stable reduced cyt *c* (right) as a function of the stronger denaturant guanidinium thiocyanate (GmSCN), used in order to minimize salt concentration in the NMR analysis. The HX rate for each measurably slow hydrogen atom was determined at each denaturant concentration by a series of 1D and 2D NMR spectra (pDr 7, 30 °C). From each rate, the free energy for the dominant opening reaction (ΔG_{HX}) was computed using equation (1) and calculable free peptide rates.

The slope of the curve for each hydrogen, expressed by the *m* value ($m = -\Delta\Delta G_{HX}/\Delta$[denaturant]), provides a measure of the denaturant-sensitive surface exposed in the opening reaction that dominates its exchange. At low denaturant neighboring NH protons often exchange at very different rates and show *m* values near zero, indicating exchange by way of different small fluctuations with little new surface exposure. When denaturant is increased, larger unfoldings that were previously invisible are sharply promoted (large *m* values) and come to dominate the exchange of the many hydrogens that they expose.

Global unfolding: the blue N/C helix unit

Figure 2(a) and (b) show the amide NH protons in the N-terminal helix and Figure 2(c) and (d) the C-terminal helix. Many NH groups in both terminal helices exchange through local fluctuations ($m \sim 0$) at low denaturant, but they all become dominated by the blue isotherm when it is sufficiently promoted by increasing denaturant. The blue HX isotherm merges smoothly with circular dichroism data for the global unfolding transition measured at high GmCl (Bai *et al.*, 1994) and at high temperature (see Figure 6(c)) indicating that it represents the global unfolding reaction.

In oxidized cyt *c*, the NH protons of residues 94 through 99 in the C-helix act as markers that exchange only with the global unfolding isotherm (above 0.7 M GmCl). The HX data indicate a global ΔG of 12.8 kcal/mol for oxidized cyt *c* at zero GmCl (pDr7, 30 °C; Figure 2(c)). There is some spread in the ΔG values estimated by the different NH protons, suggesting a low level of protection or acceleration for different NH proton in the open state. In the much more stable reduced cyt *c*, the Leu98 NH protons continues to act as a global unfolding marker and is slowed by over 5 kcal/mol. HX rate determinations at pDr 7, 8 and 9 (Figure 2(b), (d) and (f)) demonstrate that these slowest hydrogen atoms exchange by an EX2 mechanism (Hvidt & Nielsen, 1966) in the region

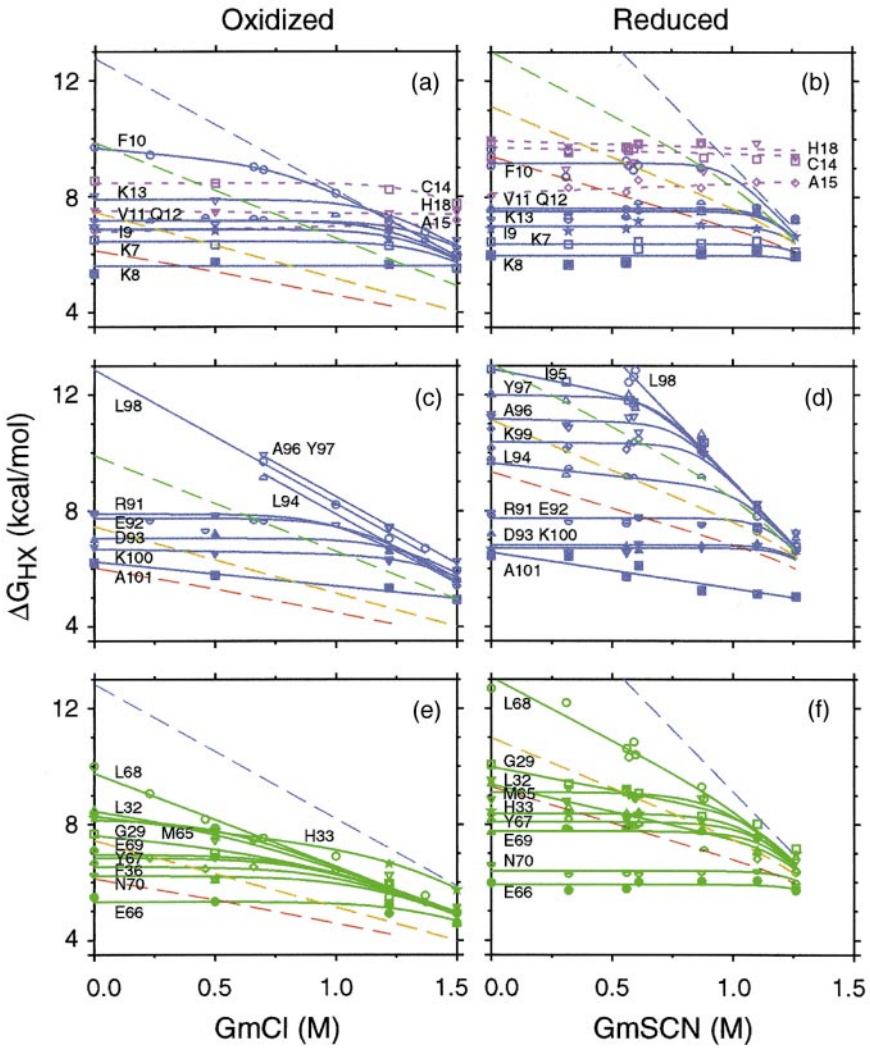

Figure 2. HX of amide NH protons in the (a)-(d) blue and (e), (f) green structural units as a function of denaturant. Free energies of the determining opening reactions were computed as in equation (1) and fit to the denaturant dependence using equations (2) and (4). The colors key the residue NH protons to their segment of origin, as shown in Figure 1. Broken lines show the HX isotherms. HX data mainly refer to p^2Hr 7 at 30 °C; multiple data points at a given condition for very slowly exchanging NH protons were at p^2Hr 7, 8 and 9 to test for EX2 behavior. (The results for oxidized cyt *c* were shown before (Bai *et al.*, 1995b)).

measured, justifying the ΔG_{HX} calculations made here.

The other NH protons that act as global unfolding markers in oxidized cyt *c* are also slowed in reduced cyt c but by less than 5 kcal (Figure 2(d)). They find high lying local fluctuational pathways that support faster exchange than the global isotherm would provide. Just as destabilization enhances and thus reveals previously hidden large unfoldings, stabilization suppresses the large unfoldings and unmasks local pathways.

The hydrogen atoms in the blue unit remain protected when the lower-lying subglobal unfolding units, which account for the rest of the protein, unfold (see below). This suggests a partially folded state with only the N and C-terminal helices formed. A kinetic folding intermediate with just this structure has been identified by HX pulse labeling (Roder *et al.*, 1988; Elöve & Roder, 1991; Sosnick *et al.*, 1994).

Within the C-terminal helix (residues 86 to 104), the well-buried non-marker NH protons of residues 94, 95, and 101 show *m* values measurably greater than zero even at low denaturant, indicating that their exchange involves a sizeable distortion of local structure. The small slope for Ala101 appears to detect a low level of helix fraying ($\sim 10^{-4}$) that reaches in from the protein's C terminus and entrains Lys99 at higher temperature (see Figure 6(c)). The slope for Leu94 and Ile95 may represent a similar fraying at the helix N terminus.

Three residues at the end of the N-terminal helix (Cys14, Ala15, His18) continue to exchange through local fluctuations ($m = 0$) from the native state even when the transient global unfolding reaction comes to dominate the exchange of all the other hydrogen atoms. This behavior, seen for

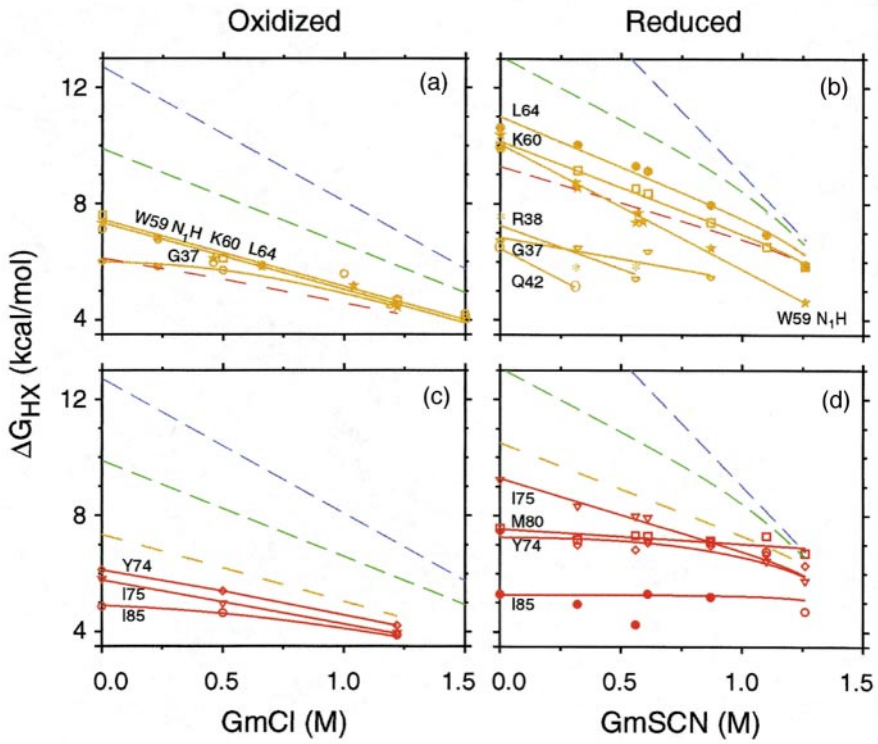

Figure 3. HX of NH protons in the (a), (b) yellow and (c), (d) red structural units. Details are as described in the legend to Figure 2.

oxidized and reduced cyt *c* (Figure 2(a) and (b)), is due to protection by residual structure in the U state. The residual structure must include the His18 heme ligand, the small loop that is covalently attached to the heme (Cys14 to Cys17), and apparently other residues acting as H-bond acceptors.

Subglobal unfolding: the green unit

Figure 2(e) and (f) show the hydrogen atoms that identify the green cooperative unfolding. All of the slow NH protons in the 60s helix (residues 65 to 70) join the green isotherm in oxidized cyt *c* and also in reduced cyt *c* so far as can be determined. Thus the entire 60s helix unfolds as a cooperative unit, like the N/C helix pair.

An omega loop at the right of cyt *c* (Figure 1) extends from the end of the N-terminal helix to Phe36 (Leszczynski & Rose, 1986). Four NH groups in the loop were measured (G29, L32, H33, F36). When denaturant is increased, the NH groups of residues 29, 32, and 36 merge into the green isotherm, suggesting that the green cooperative unfolding includes this segment also. The 60s helix and the right loop are far apart in the sequence (Figure 1), but they interact in the protein core. The unfolding of one may destabilize the other.

The His33 NH proton crosses the green isotherm in oxidized cyt c and perhaps even the global isotherm, indicating some continued protection in the unfolded segment. The determining factor may be the continued H-bonding of the His33 NH group to the Asn31 side-chain CO group as in the native protein, a local configuration that is precisely analogous to a beta bend. In reduced cyt *c* the His33 NH group merges into the greatly stabilized green isotherm.

At low denaturant the *m* values for residues 29 and 32 in the green loop are not zero, especially obvious in the reduced protein, suggesting a dependence on some small unfolding or an additional exposure reaction rather than fluctuational H-bond opening alone.

Subglobal unfolding: the yellow unit

Four measurably slow NH groups are H-bonded at the neck of a large omega loop that forms the bottom of the cyt c protein (yellow in Figure 1). The indole N_1H of Trp59 and the amide NH protons of Lys60 and Leu64 exchange together in oxidized cyt *c*, with a significant slope. The Gly37 NH proton merges with them (Figure 3(a)). The large *m* value of the merged isotherm suggests a cooperative unfolding of the entire yellow loop (Bai *et al.*, 1995b).

In reduced cyt *c* (Figure 3(b)) the yellow markers, Lys60 and Leu64, behave like the other markers, increasing in ΔG by just over 3 kcal/mol and in *m* value by the standard factor for GmSCN compared to GmCl (2.0(±0.2)). The large *m* value continues to suggest a large unfolding reaction involving the entire yellow loop segment, although these two marker NH protons separate somewhat

in ΔG, apparently due to some slowing or acceleration in the unfolded state.

The change in redox state produces structure changes through the yellow loop region (Banci *et al.*, 1997; Berghuis & Brayer, 1992; Feng *et al.*, 1990; Qi *et al.*, 1996) and anomalies appear in the HX data. Especially the Trp59 indole NH shows odd behavior. It exchanges with the same opening ΔG as Leu60 at low denaturant, but is remarkably accelerated with an aberrantly large *m* value when denaturant increases. This, together with similar anomalies in Trp59 temperature dependence (below) and perhaps also the large m values of residues 38 and 42, suggest some complex unfolding behavior within the yellow loop region.

Subglobal unfolding: the red unit

Tyr74, Ile75 and Ile85 are H-bonded at the neck of an omega loop on the left side of cyt *c* (red in Figure 1). In oxidized cyt *c*, the Tyr74 and Ile75 NH protons exchange together, with non-zero *m* value, and the Ile85 NH group merges into the same isotherm, indicating a sizeable unfolding reaction (Figure 3(c)). Also the Met80-S to heme iron ligation breaks in the same unfolding (Xu *et al.*, 1998). The concerted behavior of these four residues points to a cooperative unfolding of the red omega loop. In the more stable reduced cyt *c* (Figure 3(d)), Ile75 is slowed but remains isothermal, with the standard 3.2 kcal/mol increase in ΔG, and Tyr74 merges with the Ile75 isotherm. The Met80-S ligation to the heme iron breaks with the red unfolding in reduced as well as in oxidized cyt *c*(Xu *et al.*, 1998). Evidently the red loop unfolds as a cooperative unit in reduced as well as in oxidized cyt *c*.

The Met80 NH proton, in the red loop, shows some special behavior in reduced cyt *c*. It crosses over all the isotherms including the global isotherm, indicating continued protection in all unfolded states, like the behavior seen for the heme loop residues (Figure 2(a) and (b)) and His33 (Figure 2(e)). The protection of the Met80 NH group in the unfolded state may be due to continued H-bonding to the side-chain CO of Thr78, as in the native protein. The main-chain to side-chain H-bond mimics a beta bend, as for the His33 to Asn31 pair.

Dependence of HX rates on the redox state

The addition of a single electron to reduce the buried heme iron greatly increases the global stability of cyt *c* (Bhuyan *et al.*, 1991; Bixler *et al.*, 1992; Cohen & Pielak, 1995; Hilgen-Willis *et al.*, 1993; Komar-Panicucci *et al.*, 1994; Lo *et al.*, 1995) due to the strengthened Met80-S to heme iron ligation (Margalit & Schejter, 1973; Xu *et al.*, 1998) and additional effects in the unfolded state (Cohen & Pielak, 1995). The differences in ΔG_{HX} at 30 °C (Figures 2 and 3) are shown in Figure 4(a). To detect more of the faster NH protons a similar comparison was made at 20 °C (Figure 4(b)).

NH protons may exchange faster in oxidized cyt *c* because the positive charge on the buried heme iron promotes the OH^- - catalyzed HX reaction by an electrostatic effect. Figure 5 plots the redox-dependent change found for each NH (20 °C, pDr 7, no denaturant) against the electrostatic potential at the native state NH position due to the positively charged heme iron, computed using DelPhi (Sharp & Honig, 1990). Large redox-dependent effects are seen for residues that are attached to the heme or are close to the heme in space (seen also for cyt *c*2; Gooley *et al.*, 1991). These are shown in gray in Figure 4. As noted before, hydrogen atoms in the yellow loop also show significant changes in reduced cyt *c*, evidently due to structure changes in this region. A study of protease sensitivity found sites in the yellow loop with a difference of 36-fold in rate between oxidized and reduced cyt *c* (Wang & Kallenbach, 1998), corresponding to

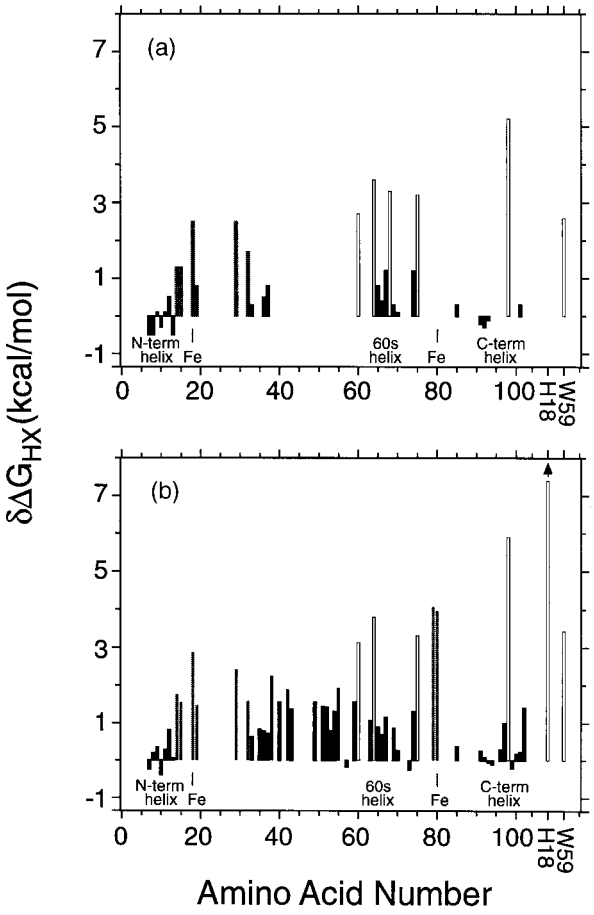

Figure 4. The change in opening free energy (reduced - oxidized) at (a) 30 °C and (b) 20 °C. The three major helices and two axial ligands of the heme iron (His18 and Met80) are indicated. Two side-chain protons are at the right. Marker protons are shown as open bars. NH protons greatly affected by heme electrostatic effects (shown in Figure 5) are in gray.

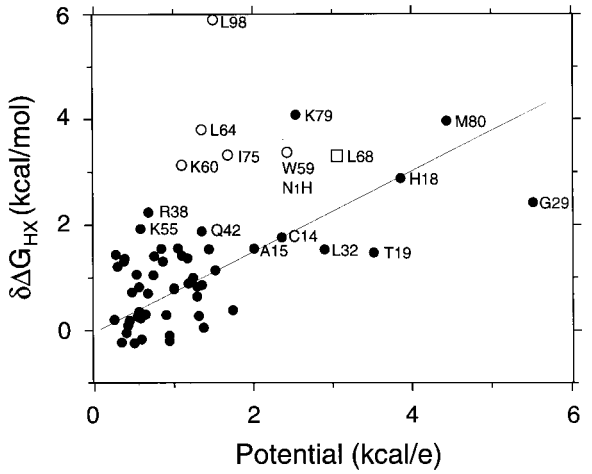

Figure 5. The change in opening free energy (as shown in Figure 4) compared to the electrostatic potential at the native state proton position. Open symbols represent marker protons. Data are at 20 °C except for Leu68 where only the 30 °C result was available. Potential at each NH proton was calculated from the X-ray model (1HRC,PBB) (Bushnell *et al.*, 1990) using DelPhi with dielectric constants of four (internal) and 20 (external). A simple $1/r$ potential gives the same picture. The diagonal places a simple electrostatic effect.

2 kcal/mol on the present scale, consistent with the moderate HX changes (Figure 4).

A major conclusion from Figures 4 and 5 is that the large HX change seen for the marker protons (open symbols) is neither electrostatic nor structure-change dependent. The marker NH protons all show large and nearly equivalent redox-dependent changes, equal to the change in stability of the Met80-S to heme iron ligation (3.2 kcal/mol). This can be expected for unfolding of the red loop which contains Met80. The fact that the same effect is also seen for the yellow and green markers provides evidence that these higher energy unfoldings include the unfolding of the red loop, just as expected for a sequential unfolding and refolding pathway (Xu *et al.*, 1998).

For present purposes, we focus on the fact that the large unfoldings are most sensitive to the stability change and that their identity is essentially unchanged in spite of the large change in stability.

Dependence of HX rates on temperature

Figure 6 shows the dependence of HX rate on temperature for the relatively slow NH protons that could be resolved by 1D NMR after simplification of the spectra by some exchange in ^2H_2O (pDr 7, no GmCl). The slope of each curve gives the entropy for the structural opening reaction that permits exchange of the hydrogen, according to $\Delta\Delta G_{HX}/\Delta T = -\Delta S_{HX}$. Opening enthalpy at any temperature can then be obtained as $\Delta H_{HX} = \Delta G_{HX} + T\Delta S_{HX}$.

For oxidized cyt *c*, a short extrapolation of the blue isotherm into the thermal transition region ($T_m = 87$ °C) closely fits melting data obtained by circular dichroism (Figure 6(c)). A similar comparison between denaturant-dependent HX and the denaturant-induced global transition found similarly good agreement (Bai *et al.*, 1994). These results confirm that the blue HX isotherm measures the global unfolding reaction. The HX data estimate the increase in global ΔG_{HX} for reduced cyt *c* at 5.2 kcal/mol at 30 °C and 5.9 kcal/mol at 20 °C (equine cyt *c*, pD_r 7, no denaturant). This increase includes the 3.2 kcal stabilization of the Met80-S to heme iron ligation in reduced cyt *c* (Xu *et al.*, 1998) and in addition 2 to 3 kcal/mol, apparently due to the neutralization of the buried heme charge (Cohen & Pielak, 1995).

Thermodynamic parameters obtained under native conditions for the global unfolding and other opening reactions are listed in Table 1. The protons identified as markers for the large unfoldings at lower temperature show a large dependence on temperature and are well-behaved out to

Table 1. Thermodynamic parameters for oxidized and reduced equine cyt *c*

	Oxidized			Reduced		
	ΔG	ΔH	TΔS	ΔG	ΔH	TΔS
A. *Blue group*						
Leu98	**0**	**120**	**120**	**0**	**160**	**160**
(at T_m)						
Leu98	**14**	**37**	**23**	**19**		
(20 °C)						
Ile9	7	14	7	7	16	9
Phe10	11	42	31	11	25	14
Val11	7	13	6	7	8	1
Glu92	8	20	12	8	14	6
Asp93	7	15	8	8	15	7
Leu94	11	42	31	9	10	1
Ala96	12	18	6	11	18	7
Tyr97				13	27	14
Lys99	10	15	5			
B. *Green group*						
Leu68	**11**	**52**	**41**			
Leu32	8	24	16	10	15	5
Met65	9	27	18	10	15	5
Tyr67	7	18	11	9	9	0
C. *Yellow group*						
Leu64	**8**	**20**	**12**	**12**	**25**	**13**
Lys60				**11**	**33**	**22**
Trp59						
N_1H	**8**	**25**	**17**	**11**	**31**	**20**
Phe36	6	15	9	7	11	4
Gly37				7	7	0
D. *Red group*						
Ile75	**6**	**18**	**12**	**9**	**20**	**11**
Tyr74				8	8	0

Marker protons are in boldface. The parameters are in kcal/mol at 20 °C except for the global Leu98 marker at the T_m (87 °C for oxidized cyt *c* and estimated roughly at 119 °C for reduced). Only the slowest NH protons, measurable by 1D NMR at 20 °C, are shown. The values given refer specifically to structural opening reactions since the effect of temperature on the chemical exchange reaction was accounted for in the k_{ch} value used to calculate ΔG_{HX} (equation (1)). (Some previously reported results refer to 30 °C; Bai *et al.*, 1995b; Xu *et al.*, 1998.)

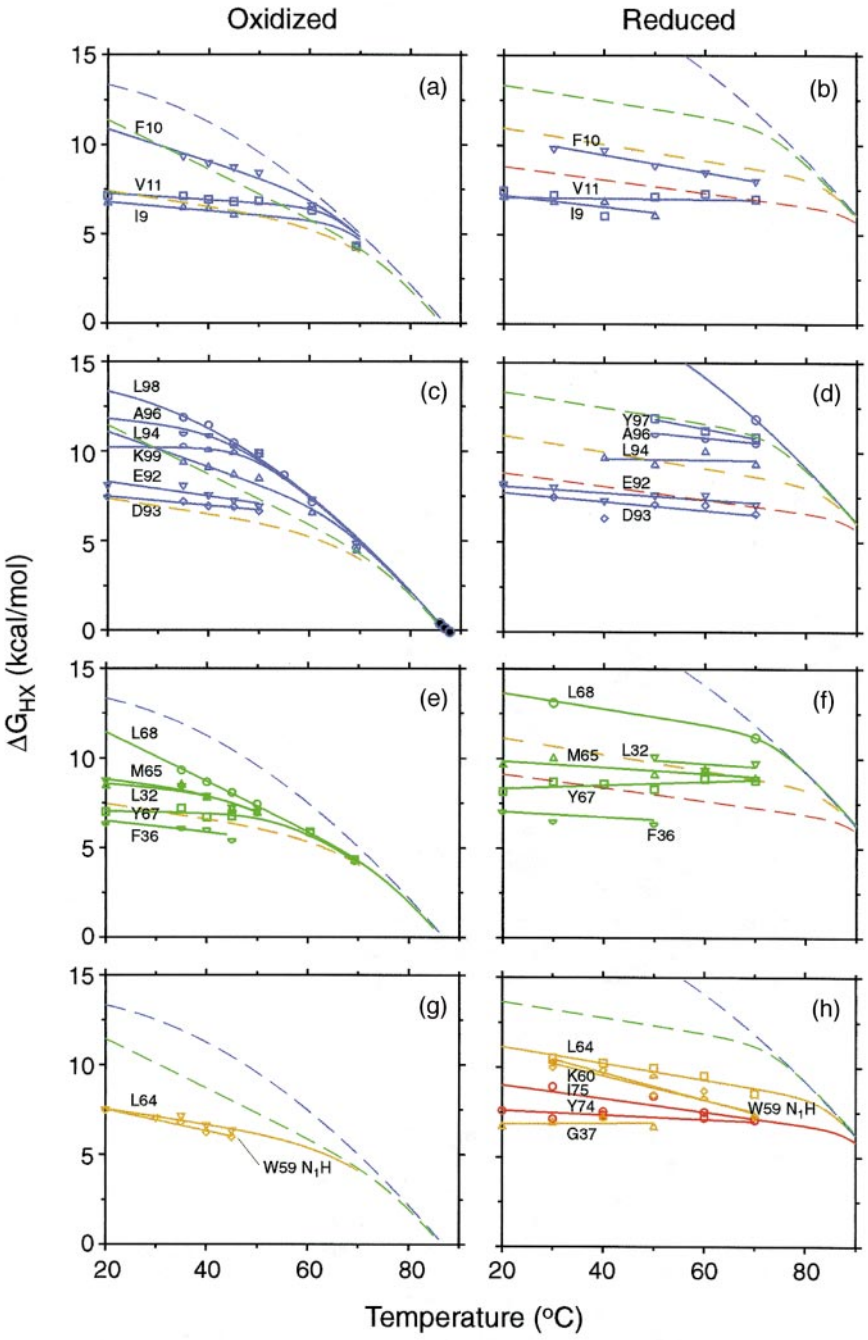

Figure 6. HX as a function of temperature. Details are as described in the legend to Figure 2. Only the slower NH protons measurable by 1D NMR are shown. Data in the global melting transition zone (filled symbols in (c)) were measured by circular dichroism.

70 °C (except for the yellow markers in reduced cyt *c*), evidently because they continue to monitor the same large unfoldings. The smaller fluctuational openings for the particularly slowly exchanging NHs measured here have lower but still significant temperature dependence.

The stability curve for global unfolding, monitored by the Leu98 marker NH group, shows significant curvature, consistent with the known ΔC_p for cyt *c* unfolding (Potekhin & Pfeil, 1989), although the temperature range studied here is insufficient to independently specify this value with good accuracy. The subglobal markers indicate that ΔC_p values are not measurably different from zero (over the temperature range measured), indicating a much smaller surface exposure than for the global folding. This is consistent with our earlier conclusion that a large surface burial in the folding transition state occurs as the first step in folding (referred to as the search-nucleation-collapse step; Sosnick *et al.*, 1996). Therefore, large

surface exposure and large ΔC_p are seen only in the last step in unfolding (blue unfolding).

Figure 7 is an enthalpy - entropy compensation plot of the results in Table 1. Surprisingly, the HX results describe a consistent curve ($r = 0.98$) with the local fluctuations and larger unfoldings on the same line. This suggests that the entropy and enthalpy of H-bond openings are linearly related, as considered by Hilser & Freire (1996), and that a relationship close to that for unfolding reactions, which is predicated on surface exposure, may hold also for the more local fluctuations even though they appear to expose little denaturant-sensitive surface. We have no explanation for this observation.

Discussion

The native state HX approach exploits the ability of stabilizing and destabilizing influences to selectively suppress or enhance the equilibium population of different kinds of high energy protein forms. The results shown here further document the HX measurement in cyt *c* of many small fluctuational openings, several distinct subglobal unfoldings, and the single global unfolding. These were recognized and characterized by their differing sensitivities to denaturant and temperature and to a localized redox change that greatly changes the protein stability. The same unfoldings are robustly maintained and well behaved over a wide range of temperatures and denaturant concentrations and through the redox transition.

Detection of large unfoldings

Small fluctuational openings and larger unfoldings often have similarly high apparent free energy so that the dominant HX mechanism cannot be distinguished on the basis of exchange rate alone. They can be distinguished by their differing sensitivity to destabilizing influences. Denaturant (Bai *et al.*, 1995a; Chamberlain *et al.*, 1996; Hiller *et al.*, 1997; Fuentes & Wand, 1998a), temperature (Bai *et al.*, 1995a), and pressure (Fuentes & Wand, 1998b) have been exploited to selectively promote large unfoldings so that they come to dominate the exchange of the residue NH protons that they expose. The present results extend these demonstrations.

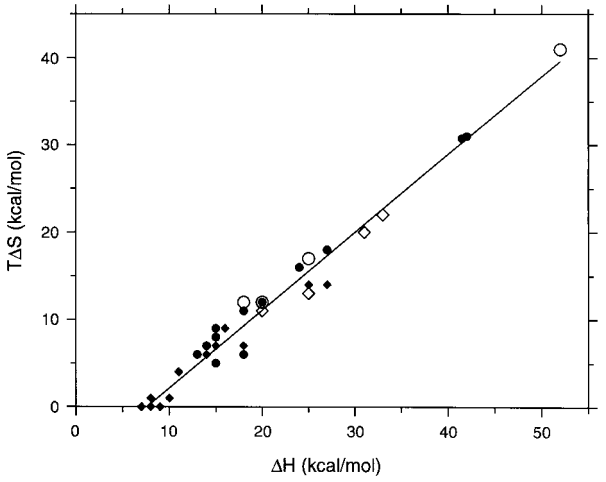

Figure 7. Enthalpy - entropy compensation plot (data in Figure 6 and Table 1). Temperature was taken as 293°K. The different symbols distinguish marker and non-marker protons in oxidized and reduced cyt *c*.

Certain constraints limit the ability of native state HX to uncover and define large unfoldings. The number of slowly exchanging NH probes is important. Helices and β-strands have many; loops have few. The dynamic range in *m* and ΔG_{HX} that is available for resolving different HX isotherms is limited by the protein's size and stability. Small size may lead to unuseably small *m* values; small stability will obscure subglobal unfoldings that are at higher free energy than the global unfolding. For example, the small CI2 protein (67 residues) resists dissection by native state HX (Itzhaki *et al.*, 1997), perhaps because of these limitations. Stability that is too great may interfere as does stability that is too small. For example, in reduced cyt *c* the large unfoldings are suppressed much more than the local fluctuations. Some of the local fluctuational HX curves then fail to merge definitively into their particular unfolding isotherms before the different isotherms themselves draw together. Another constraint is illustrated by barnase. The slow refolding of barnase produces an EX1 condition when it is mildly destabilized. This complicates the search for subglobal unfoldings (Clarke & Fersht, 1996), although the EX1 condition may be usefully exploited to determine unfolding rates (Loh *et al.*, 1996; Arrington & Robertson, 1977).

It is noteworthy that sizeable denaturant-dependent *m* values may occur in the absence of large cooperative unfolding reactions. Cases seen here include fraying behavior, H-bond breaking fluctuations of well-buried NH groups that require some additional distortion, and some fluctuations within omega loops. In general, however, the two extreme types of openings, small local fluctuations and large unfoldings, are dominant.

In summary, a number of factors can interfere with the experimental study of large unfolding reactions. Nevertheless, such studies have now succeeded with a number of proteins (Chamberlain *et al.*, 1996; Fuentes & Wand, 1998a,b; Hiller *et al.*, 1997) including cyt *c* (Bai & Englander, 1996; Bai *et al.*, 1995b). The present study using multiple perturbants provides further confirmation of the validity of this approach and further insight into its strengths and limitations.

Subglobal cooperativity

We are especially interested in the nature of the units that unfold and refold to produce partially unfolded intermediates. In cyt *c*, the entire N/C helix pair acts as a cooperative unfolding unit, as does the entire 60s helix. Transient cooperative unfolding of single or paired helices has also been seen in RNase H (Chamberlain *et al*., 1996) and apo cyt *b*562 (Fuentes & Wand, 1998a,b). The cooperative subglobal unfolding of entire helical segments has been measured at equilibrium in α-lactalbumin (Schulman & Kim, 1996). The fraying of terminal residues is another expression of helical cooperativity (Lifson & Roig, 1961; Zimm & Bragg, 1959).

A case of beta-strand cooperativity has been seen in ribonuclease H (Chamberlain *et al*., 1996). Cyt *c* has no clear beta sheet elements but does incorporate three omega loops. The HX results support the cooperative unfolding of the entire red loop in cyt *c* and apparently the green loop together with the 60s helix. The entire yellow loop in both oxidized and reduced cyt *c* appears to unfold as a cooperative unit (from the marker residues 60 and 64), although it adopts additional unexplained sub-loop characteristics in reduced cyt *c*. The cooperative unfolding of omega loops presumably depends on the fact that they are self-contained units that tend to pack their side-chains internally, making many self contacts (Leszczynski & Rose, 1986).

All of these results consistently suggest that the secondary structural elements that make up a protein molecule act as cooperative unfolding units. The intrinsic cooperativity of isolated helices has long been known (Linderstrøm-Lang & Schellman, 1959, Zimm & Bragg, 1959; Lifson & Roig, 1961). Apparently, omega loops and beta sheets or segments thereof also unfold and refold as cooperative units. Tertiary interactions greatly stabilize secondary structural elements and ambient conditions can greatly reduce their stability, but their cooperative nature is intrinsic to their structure and tends to be maintained. Thus it appears that protein molecules can be viewed as an accretion of a small number of interacting and mutually stabilizing cooperative elements. In latttice model terminology, proteins might be represented by a small number of beads with each bead signifying a distinct structural unit much larger than a single amino acid residue.

The folding landscape

The retention of submolecular cooperativity seen in cyt *c* and other proteins dictates that their partially unfolded forms occupy a small number of distinct wells in the conformational free energy landscape. Neighboring states in conformational space, for example with part of a given helix unfolded, are likely to be at higher free energy than for the helix either fully formed or fully unfolded.

The classical model for protein folding pictures relatively defined partially unfolded intermediates as metastable forms in sequential energy wells. Proteins fold in a stepwise manner through these intermediate forms. In contrast, the energy landscape derived from theoretical analyses of non-protein models generally pictures a continuum of overlapping, non-cooperative, partially unfolded forms. The models fold energetically downhill through the continuum by the accumulation of native-like interactions in no particular order (with some exceptions; Crippen & Ohkubo, 1998; Pande & Rokhsar, 1999). The considerations just reviewed suggest that the theoretical models appear to project continuous rather than discrete intermediates because they do not possess separate cooperative elements.

In this context it is useful to consider known molecules that possess only one cooperative unit, such as independently stable helices (Thompson *et al*., 1997) and beta hairpins (Munoz *et al*., 1997). These fold by adding one residue at a time in a downhill manner after some initial nucleation event. The order of residue addition is determined by the linear nature of these molecules. Their lattice model analogs also comprise only one cooperative unit and fold analogously, but their three-dimensional nature makes the order of residue addition arbitrary so that they appear to fold through a very large number of continuously distributed intermediates and pathways. In a successful native state HX investigation (see limitations above), proteins that behave in this way would show many large-scale partially unfolded states. The NH protons of near neighbor residues might exchange by way of a continuum of progressively larger unfoldings or even by very different large unfoldings (Miller & Dill, 1995), perhaps as suggested by the exceptional behavior of the yellow loop in reduced cyt *c* (Figure 3(b)). In general, this is not what HX experiments find. Rather, the amide NH protons in distinct structural units are seen to group into a few discrete HX isotherms that depict a small number of discrete intermediates.

In summary, experimental results show that proteins composed of multiple cooperative elements unfold (and refold) in pieces, producing metastable, native-like, partially folded intermediate forms that identify distinct wells in the folding reaction landscape. Simple molecules and non-protein models that do not encompass separate cooperative units can be expected to behave differently. They appear, in simulations, to unfold and refold in a more continuous manner, reflecting the continuous more or less monotonic traverse between the U or N state and the transition state between them. It is important to note that these conclusions are drawn from HX experiments performed under equilibrium native conditions and therefore refer to the shape of the reaction landscape at equilibrium. A demonstration that the equilibrium PUFs observed serve as kinetic intermediates in folding

pathways is not necessary for the conclusions reached. It is noteworthy, however, that a quantity of available evidence does implicate these very same PUFs as kinetic folding intermediates (see e.g. Englander, 1998).

Materials and Methods

Horse heart cyt *c* (type VI) was from Sigma Chemical Co, ^2H_2O from Isotec, and GmSCN from ICN. All other chemicals were reagent grade. Buffers used were 0.1 M phosphate at pD_r 7.0 - 8.5 and 0.1 M pyrophosphate at p^2Hr 9. (pDr is the pH meter reading uncorrected for the ^2H_2O effect.)

NMR measurements and data analysis were as previously described (Bai *et al*., 1995a; Milne *et al*., 1998; Xu *et al*., 1998). Thermal melting experiments using circular dichroism were done one temperature point at a time to avoid the progressive development of irreversibly denatured material.

Hydrogen exchange

The free energy of the opening reaction (ΔG_{op}) that leads to exchange of each hydrogen was obtained from:

$$\Delta G_{HX} = -RT \ln K_{op} = -RT \ln(1/P) = -RT \ln(k_{ch}/k_{ex}) \quad (1)$$

K_{op} is the equilibrium constant of the controlling opening reaction, obtained from the measured HX protection factor (P), which is defined by the ratio of the exchange rate for each hydrogen atom (k_{ex}) and its intrinsic chemical exchange rate (k_{ch}) under the conditions used. The relationships in equation (1) hold in the usual EX2 case where reclosing is faster than k_{ch} (Englander & Kallenbach, 1984; Hvidt & Nielsen, 1966). The k_{ch} value for each residue NH proton when it is freely exposed to solvent under the same conditions can be calculated (Bai *et al*., 1993; Connelly *et al*., 1993).

HX data as a function of temperature or denaturant under native conditions were fit by equation (2) together with the pertinent expression from equations (3) and (4):

$$\begin{aligned}\Delta G_{HX} &= -RT \ln(K_{op,1} + K_{op,s} + K_{op,g}) \\ &= -RT \ln[\exp(-\Delta G_l/RT) + \exp(-\Delta G_s/RT) \\ &\quad + \exp(-\Delta G_g/RT)]\end{aligned} \quad (2)$$

The subscripts indicate local (l), subglobal (s), and global (g) openings. Equations (3) and (4) describe the stability of a protein as a function of temperature and denaturant:

$$\Delta G(T) = \Delta H_m - T\Delta S_m + \Delta C_p[(T - T_m) - T \ln(T/T_m)] \quad (3)$$

$$\Delta G(\text{den}) = \Delta G(0) - m[\text{den}] \quad (4)$$

Parameters are the enthalpy (ΔH_m) and entropy (ΔS_m) of an unfolding transition, referenced here to its midpoint melting temperature (T_m), the difference in partial specific heat between the native and unfolded forms (ΔC_p), and the m value for denaturant-driven unfolding which in many cases proportions to the newly exposed denaturant sensitive surface (Pace, 1975). A ΔC_p value of 1.3 kcal/mol/K (Potekhin & Pfeil, 1989) was used for the global marker (Leu98 NH) and was zero otherwise.

Acknowledgements

This work was supported by NIH research grant GM31845 and a grant from the Mathers Charitable Foundation.

References

Arrington, C. B. & Robertson, A. D. (1997). Microsecond protein folding kinetics from native state hydrogen exchange. *Biochemistry,* **36**, 8686-8691.

Bai, Y. & Englander, S. W. (1996). Future directions in folding: the multi-state nature of protein structure. *Proteins: Struct. Funct. Genet.* **24**, 145-151.

Bai, Y., Milne, J. S., Mayne, L. & Englander, S. W. (1993). Primary structure effects on peptide group hydrogen exchange. *Proteins: Struct. Funct. Genet.* **17**, 75-86.

Bai, Y., Milne, J. S., Mayne, L. & Englander, S. W. (1994). Protein stability parameters measured by hydrogen exchange. *Proteins: Struct. Funct. Genet.* **20**, 4-14.

Bai, Y., Englander, J. J., Mayne, L., Milne, J. S. & Englander, S. W. (1995a). Thermodynamic parameters from hydrogen exchange measurements. *Methods Enzymol.* **259**, 344-356.

Bai, Y., Sosnick, T. R., Mayne, L. & Englander, S. W. (1995b). Protein folding intermediates studied by native state hydrogen exchange. *Science,* **269**, 192-197.

Banci, L., Bertini, I., Gray, H. B., Luchinat, C., Reddig, T., Rosato, A. & Turano, P. (1997). Solution structure of oxidized horse heart cytochrome *c*. *Biochemistry,* **36**, 9867-9877.

Berghuis, A. M. & Brayer, G. D. (1992). Oxidation state-dependent conformational changes in cytochrome *c*. *J. Mol. Biol.* **223**, 959-976.

Bhuyan, A. K., Elöve, G. A. & Roder, H. (1991). Redox effects on protein stability and folding kinetics of horse cytochrome *c*. *J. Cell. Biochem.* **Suppl. 15G**, 188.

Bixler, J., Baker, G. & McLendon, G. (1992). Electrochemical probes of protein folding. *J. Am. Chem. Soc.* **114**, 6938-6939.

Bryngelson, J. D., Onuchic, J. N., Socci, N. D. & Wolynes, P. G. (1995). Funnels, pathways, and the energy landscape of protein folding: a synthesis. *Proteins: Struct. Funct. Genet.* **21**, 167-195.

Bushnell, G. W., Louie, G. V. & Brayer, G. D. (1990). High-resolution three dimensional structure of horse heart cytochrome *c*. *J. Mol. Biol.* **213**, 585-595.

Chamberlain, A. K., Handel, T. M. & Marqusee, S. (1996). Detection of rare partially folded molecules in equilibrium with the native conformation of RNaseH. *Nature Struct. Biol.* **3**, 782-787.

Clarke, J. & Fersht, A. R. (1996). An evaluation of the use of hydrogen exchange at equilibrium to probe intermediates on the protein folding pathway. *Folding Design,* **1**, 243-254.

Cohen, D. S. & Pielak, G. J. (1995). Entropic stabilization of cytochrome *c* upon reduction. *J. Am. Chem. Soc.* **117**, 1675-1677.

Connelly, G. P., Bai, Y., Jeng, M.-F., Mayne, L. & Englander, S. W. (1993). Isotope effects in peptide group hydrogen exchange. *Proteins: Struct. Funct. Genet.* **17**, 87-92.

Creighton, T. E. (1990). Protein folding. *Biochem. J.* **270**, 1-16.

Crippen, G. M. & Ohkubo, Y. Z. (1998). Statistical mechanics of protein folding by exhaustive enumeration. *Proteins: Struct. Funct. Genet.* **32**, 425-437.

Dill, K. A. & Chan, H. S. (1997). From Levinthal to pathways to funnels. *Nature Struct. Biol.* **4**, 10-19.

Elöve, G. A. & Roder, H. (1991). Structure and stability of cytochrome *c* folding intermediates. In *Protein Refolding* (Georgiou, G. & De Bernardez-Clark, E., eds), pp. 50-63, ACS Symposium Series, Washington DC.

Englander, S. W. (1998). Native state HX. *Trends Biochem. Sci.* **23**, 378.

Englander, S. W. & Kallenbach, N. R. (1984). Hydrogen exchange and structural dynamics of proteins and nucleic-acids. *Quart. Rev. Biophys.* **16**, 521-655.

Feng, Y., Roder, H. & Englander, S. W. (1990). Redox-dependent structure change and hyperfine NMR shifts in cytochrome *c*. *Biochemistry,* **29**, 3494-3504.

Fuentes, E. J. & Wand, A. J. (1998a). Local dynamics and stability of apocytochrome b_{562} examined by hydrogen exchange. *Biochemistry,* **37**, 3687-3698.

Fuentes, E. J. & Wand, A. J. (1998b). The local stability and dynamics of apocytochrome b_{562} examined by the dependence of hydrogen exchange on hydrostatic pressure. *Biochemistry,* **37**, 3687-3698.

Gooley, P. R., Zhao, D. & MacKenzie, N. E. (1991). Comparison of amide proton exchange in reduced and oxidized *Rhodobacter capsulatus* cytochrome *c*2: a 1H-15N study. *J. Biomol. NMR,* **1**, 145-154.

Hilgen-Willis, S., Bowden, E. F. & Pielak, G. J. (1993). Dramatic stabilization of ferricytochrome *c* upon reduction. *J. Inorg. Biochem.* **51**, 663-676.

Hiller, R., Zhou, Z. H., Adams, M. W. W. & Englander, S. W. (1997). Stability and dynamics in a hyperthermophilic protein with melting temperature close to 200 °C. *Proc. Natl Acad. Sci. USA,* **94**, 11329-11332.

Hilser, V. J. & Freire, E. (1996). Structure-based calculation of the equilibrium folding pathway of proteins. Correlation with hydrogen exchange protection factors. *J. Mol. Biol.* **262**, 756-772.

Hvidt, A. & Nielsen, S. O. (1966). Hydrogen exchange in proteins. *Advan. Protein Chem.* **21**, 287-386.

Itzhaki, L. S., Neira, J. L. & Fersht, A. R. (1997). Hydrogen exchange in chymotrypsin inhibitor 2 probed by denaturants and temperature. *J. Mol. Biol.* **270**, 89-98.

Kim, P. S. & Baldwin, R. L. (1982). Specific intermediates in the folding reactions of small proteins and the mechanism of protein folding. *Annu. Rev. Biochem.* **51**, 459-489.

Kim, P. S. & Baldwin, R. L. (1990). Intermediates in the folding reactions of small proteins. *Annu. Rev. Biochem.* **59**, 631-660.

Komar-Panicucci, S., Weis, D., Bakker, G., Qiao, T., Sherman, F. & McLendon, G. (1994). Thermodynamics of the equilibrium unfolding of oxidized and reduced Saccharomyces cerevisiae iso-1-cytochromes *c*. *Biochemistry,* **33**, 10556-10560.

Leszczynski, J. F. & Rose, G. D. (1986). Loops in globular proteins: a novel category of secondary structure. *Science,* **234**, 849-855.

Lifson, S. & Roig, A. (1961). On the theory of the helix-coil transion in polypeptides. *J. Chem. Phys.* **34**, 1963-1974.

Linderstrøm-Lang, K. & Schellman, J. A. (1959). Protein structure and enzyme activity. In *The Enzymes* (Boger, P. D., Lardy, H. & Myrback, K., eds), 2nd edit; pp. 443-510, Academic Press, New York.

Lo, T. P., Komar-Panicucci, S., Sherman, F., McLendon, G. & Brayer, G. D. (1995). Structural and functional effects of multiple mutations at distal sites in cytochrome *c*. *Biochemistry,* **34**, 5259-5268.

Loh, S. N., Rohl, C. A., Kiefhaber, T. & Baldwin, R. L. (1996). A general two-process model describes the hydrogen exchange behavior of RNase A in unfolding conditions. *Proc. Natl Acad. Sci. USA,* **93**, 1982-1987.

Margalit, R. & Schejter, A. (1973). Cytochrome *c*: a thermodynamic study of the relationships among oxidation state, ion-binding and structural parameters. 1. The effects of temperature, pH and electrostatic media on the standard redox potential of cytochrome *c*. *Eur. J. Biochem.* **32**, 492-499.

Miller, D. W. & Dill, K. A. (1995). A statistical mechanical model for hydrogen exchange in globular proteins. *Protein Sci.* **4**, 1860-1873.

Milne, J. S., Mayne, L., Roder, H., Wand, A. J. & Englander, S. W. (1998). Determinants of protein hydrogen exchange studied in equine cytochrome *c*. *Protein Sci.* **7**, 739-745.

Mirny, L. A., Abkevich, V. & Shakhnovich, E. I. (1996). Universality and diversity of folding scenarios: a comprehensive analysis with the aid of a lattice model. *Fold. Design,* **1**, 103-116.

Munoz, V., Thompson, P. A., Hofrichter, J. & Eaton, W. A. (1997). Folding dynamics and mechanism of beta-hairpin formation. *Nature,* **390**, 196-199.

Pace, C. N. (1975). The stability of globular proteins. *CRC Crit. Rev. Biochem.* **3**, 1-43.

Parde, V. S. & Rokhsar, D. S. (1999). Folding pathway of a lattice model for proteins. *Proc. Natl Acad. Sci. USA,* **96**, 1273-1278.

Potekhin, S. & Pfeil, W. (1989). Microcalorimetric studies of conformational transitions of ferricytochrome *c* in acidic solution. *Biophys. Chem.* **34**, 55-62.

Ptitsyn, O. B. (1995). Molten globule and protein folding. *Advan. Protein Chem.* **47**, 83-229.

Qi, P. X., Beckman, R. A. & Wand, A. J. (1996). Determination of solution structure and detection of redox-related structure changes of horse heart cytochrome *c* by high resolution NMR and restrained simulated annealing. *Biochemistry,* **35**, 12275-12286.

Roder, H., Elöve, G. A. & Englander, S. W. (1988). Structural characterization of folding intermediates in cytochrome c by H-exchange labeling and proton NMR. *Nature,* **335**, 700-704.

Schulman, B. A. & Kim, P. S. (1996). Proline scanning mutagenesis of a molten globule reveals non-cooperative formation of a protein's overall topology. *Nature Struct. Biol.* **3**, 682-687.

Sharp, K. A. & Honig, B. (1990). Electrostatic interactions in macromolecules: theory and applications. *Annu. Rev. Biophys. Biophys. Chem.* **19**, 301-332.

Sosnick, T. R., Mayne, L., Hiller, R. & Englander, S. W. (1994). The barriers in protein folding. *Nature Struct. Biol.* **1**, 149-156.

Thompson, P. A., Eaton, W. A. & Hofrichter, J. (1997). Laser temperature jump study of the helix $\Longleftrightarrow$ coil kinetics of an alanine peptide interpreted with a 'kinetic zipper' model. *Biochemistry,* **36**, 9200-9210.

Veitshans, T., Klimov, D. & Thirumalai, D. (1997). Protein folding kinetics: timescales, pathways and energy landscapes in terms of sequence-dependent properties. *Fold. Design,* **2**, 1-22.

Wang, L. & Kallenbach, N. R. (1998). Proteolysis as a measure of the free energy difference between cytochrome *c* and its derivatives. *Protein Sci.* **7**, 2460-2464.

Wolynes, P. G., Onuchic, J. N. & Thirumalai, D. (1995). Navigating the folding routes. *Science,* **267**, 1619-1620.

Xu, Y., Mayne, L. C. & Englander, S. W. (1998). Evidence for an unfolding and refolding pathway in cytochrome *c*. *Nature Struct. Biol.* **5**, 774-778.

Zimm, G. H. & Bragg, J. K. (1959). Theory of the phase transition between helix and random coil in polypeptide chains. *J. Chem. Phys.* **31**, 526-535.

Edited by P. E. Wright

(Received 9 April 1999; received in revised form 27 May 1999; accepted 28 May 1999)